

Phosphocaveolin-1 Enforces Tumor Growth and Chemoresistance in Rhabdomyosarcoma

Fiorella Faggi^{1,6}, Stefania Mitola¹, Guglielmo Sorci^{2,6}, Francesca Riuzzi^{2,6}, Rosario Donato^{2,6}, Silvia Codenotti^{1,6}, Pietro Luigi Poliani¹, Manuela Cominelli¹, Raffaella Vescovi¹, Stefania Rossi¹, Stefano Calza¹, Marina Colombi¹, Fabio Penna^{3,6}, Paola Costelli^{3,6}, Ilaria Perini⁴, Maurilio Sampaolesi^{4,5,6}, Eugenio Monti¹, Alessandro Fanzani^{1,6*}

1 Department of Molecular and Translational Medicine, University of Brescia, Brescia, Italy, **2** Department of Experimental Medicine and Biochemical Sciences, University of Perugia, Perugia, Italy, **3** Department of Experimental Medicine and Oncology, University of Torino, Torino, Italy, **4** Stem Cell Research Institute, University Hospital Gasthuisberg, Leuven, Belgium, **5** Human Anatomy Section, University of Pavia, Pavia, Italy, **6** Interuniversity Institute of Myology (IIM), Italy

Abstract

Caveolin-1 (Cav-1) can ambiguously behave as either tumor suppressor or oncogene depending on its phosphorylation state and the type of cancer. In this study we show that Cav-1 was phosphorylated on tyrosine 14 (pCav-1) by Src-kinase family members in various human cell lines and primary mouse cultures of rhabdomyosarcoma (RMS), the most frequent soft-tissue sarcoma affecting childhood. Cav-1 overexpression in the human embryonal RD or alveolar RH30 cells yielded increased pCav-1 levels and reinforced the phosphorylation state of either ERK or AKT kinase, respectively, in turn enhancing *in vitro* cell proliferation, migration, invasiveness and chemoresistance. In contrast, reducing the pCav-1 levels by administration of a Src-kinase inhibitor or through targeted Cav-1 silencing counteracted the malignant *in vitro* phenotype of RMS cells. Consistent with these results, xenotransplantation of Cav-1 overexpressing RD cells into nude mice resulted in substantial tumor growth in comparison to control cells. Taken together, these data point to pCav-1 as an important and therapeutically valuable target for overcoming the progression and multidrug resistance of RMS.

Citation: Faggi F, Mitola S, Sorci G, Riuzzi F, Donato R, et al. (2014) Phosphocaveolin-1 Enforces Tumor Growth and Chemoresistance in Rhabdomyosarcoma. PLoS ONE 9(1): e84618. doi:10.1371/journal.pone.0084618

Editor: Natasha Kyrianiou, University of Kentucky College of Medicine, United States of America

Received: May 28, 2013; **Accepted:** November 15, 2013; **Published:** January 10, 2014

Copyright: © 2014 Faggi et al. This is an open-access article distributed under the terms of the Creative Commons Attribution License, which permits unrestricted use, distribution, and reproduction in any medium, provided the original author and source are credited.

Funding: This work was supported by the Fondazione Cariplo grant to EM, Grant NEDD - Network Enabled Drug Design, Regione Lombardia to EM, "Associazione Italiana per la Ricerca sul Cancro" (MFAG Project n. 9161 to SM and Project 6021 to RD) and University of Brescia research fund (ex 60%) to AF and EM. The funders had no role in study design, data collection and analysis, decision to publish, or preparation of the manuscript.

Competing Interests: The authors have declared that no competing interests exist.

* E-mail: fanzani@med.unibs.it

Introduction

Caveolins (i.e. Cav-1, Cav-2 and Cav-3) are 21–24 kDa membrane-associated proteins that mainly localize in the 50–100 nm cholesterol-enriched invaginations of the plasma membrane, known as *caveolae* [1–3]. Caveolins are pivotally involved in multiple processes, including endocytosis, cholesterol homeostasis, regulation of signal transduction and *caveolae* biogenesis that requires the complementary action of Cavin family members [4–6]. Cav-1, in particular, has been shown to mostly inhibit a large number of signaling pathways because of the presence of a caveolin scaffolding domain that allows the binding of a plethora of proteins, such as epidermal growth factor receptor, protein kinases C, endothelial nitric oxide synthase [7]. In response to a variety of stimuli such as growth factors, UV irradiation, mechanical and oxidative stress, Cav-1 can also be phosphorylated on tyrosine 14 (hereafter referred as to pCav-1) by members of the sarcoma kinases (Src-kinases) [8–10], in turn leading to activation of pathways linked to cell death or survival [11]. In cancer, there is mounting evidence that pCav-1 occurrence often predicts unfavorable outcome by supporting anchorage-independent cell growth, migration, invasiveness and multidrug resistance [11–15]. Rhabdomyosarcoma (RMS) is a pediatric soft-tissue cancer [16–20] that arises from various muscle and non-muscle progenitors

characterized by interrupted myogenesis [21–28]. The current classification includes two major histological variants, known as embryonal (ERMS) and alveolar (ARMS), with the former characterized by a complex genomic aetiology [16,17] and the latter by the prevalent expression of chimeric transcription factors generated by the fusion of the paired box 3 or 7 with forkhead box O1 (Pax3-Foxo1 or Pax7-Foxo1) as a result of specific chromosomal translocations [29,30].

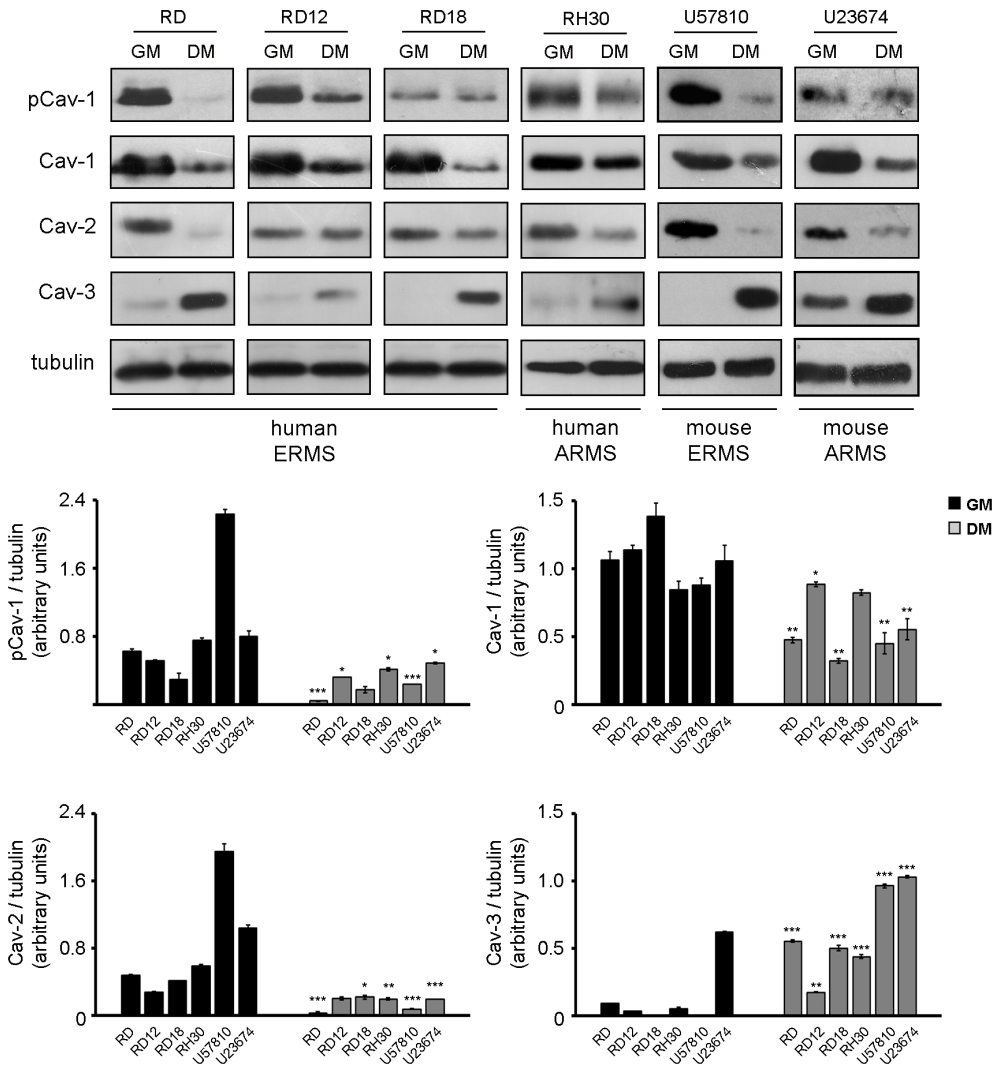
Previously we have shown that Cav-1 is consistently expressed in both the histological RMS variants [31,32]. Here, we provide further evidence that Cav-1 is consistently phosphorylated through a Src-dependent mechanism in various ERMS and ARMS cell lines, playing a pivotal role in tumor growth and chemoresistance.

Results

Cav-1 is phosphorylated through a Src-dependent mechanism in RMS cells

The expression levels of Caveolin family members were analysed by western blot using four human RMS cell lines (embryonal RD, RD12, RD18 and alveolar RH30) and two mouse primary tumor cultures established from transgenic Myf6Cre/p53^{-/-} and Myf6Cre/Pax3-Foxo1/p53^{-/-} mice (embryonal U57810 and alveolar U23674, respectively) [21,24]. In

A



B

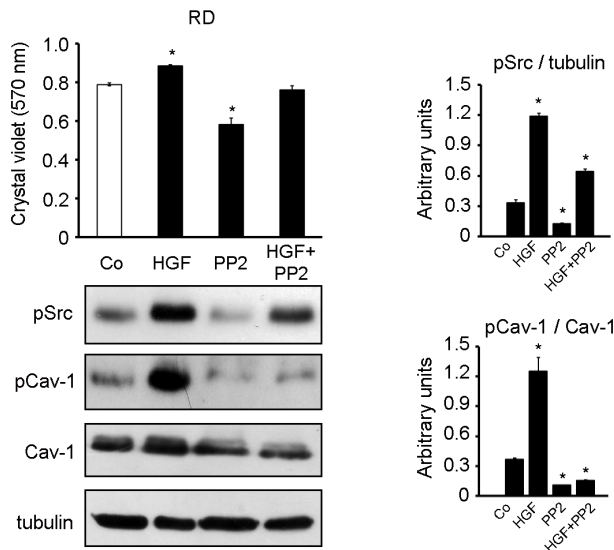


Figure 1. Expression analysis of Caveolins in RMS cells. A) Caveolin protein levels were investigated using human cell lines and mouse primary cultures. Cells were seeded in 60-mm dishes (at a density of 12×10^4) and cultured in GM until confluence, followed by incubation in DM. After 72 hours in GM or DM, cells were harvested and protein homogenates western blotted for pCav-1, Cav-1, Cav-2, Cav-3 and tubulin. Protein bands were quantified by densitometry after normalization with respect to tubulin ($n=3$). *, $P<0.05$; **, $P<0.001$; ***, $P<0.0001$. B) Human RD cells were seeded in 60-mm dishes (at a density of 15×10^4). After 24 hours, cells were treated or not with 10 ng/ml HGF for 24 hours, in the absence or presence of pre-administered 10 μ M PP2. Cells were then harvested and protein homogenates western blotted for pSrc, pCav-1, Cav-1 and tubulin. Protein bands were quantified by densitometry after normalization with respect to tubulin ($n=3$). *, $P<0.05$. After 48 hours, cell proliferation was measured by Crystal violet assay. Histograms represent means \pm SD of absorbance. ($n=4$) *, $P<0.05$. doi:10.1371/journal.pone.0084618.g001

cells maintained in a growth medium (GM) we observed co-expression of Cav-1 (both Tyr14-phosphorylated and total forms) with Cav-2 and lack or very low expression of Cav-3 (Fig. 1A). Instead, treatment of cells with a differentiation medium (DM) lead to down-regulation of both Cav-1 and Cav-2 and increased Cav-3 levels (Fig. 1A). It is well established that Cav-1 is a substrate of Src-kinase family members [8–10], which are upstream activated by different tyrosine kinase receptors involved in cell proliferation and survival upon binding with ligands such as hepatocyte growth factor (HGF), platelet-derived growth factor, insulin and insulin-like growth factor [33–37]. Thus, treatment of RD cells with HGF, a growth factor playing a pivotal role in RMS progression [38–40], elicited increasing pSrc and pCav-1 levels compared to untreated cells (Fig. 1B, western blot), in turn promoting a rise in cell proliferation (Fig. 1B, Crystal violet assay). In contrast, the effects promoted by HGF were counteracted by co-treatment with a synthetic Src-kinase inhibitor, known as PP2 (Fig. 1B), and similar results were obtained in mouse cultures (not shown). These data point to pCav-1 as a downstream target of Src-kinases especially during proliferation of RMS cells.

pCav-1 levels affect cell proliferation

To gain further insights into the role of pCav-1, we investigated the effects of Cav-1 overexpression and knockdown using the human RD and RH30 cell lines, which are widely employed as particularly representative of ERMS and ARMS histotypes, respectively [41]. As observed in two distinct clones of each cell line, Cav-1 overexpression correlated with increased pCav-1 levels (Fig. 2A, western blot), leading to a significantly faster proliferation compared to controls, as evaluated by cell counting (Fig. 2A, bottom graph). Consistently, PP2 treatment was sufficient to override the rise in cell proliferation induced by Cav-1 overexpression and to inhibit the proliferation of controls as well (Fig. 2B). In addition, cells stably transfected with a green fluorescent protein-tagged non-phosphorylatable Cav-1 form (GFP-Y14F), having pCav-1 levels comparable to parental cells (Fig. 2C), exhibited a normal cell proliferation (Fig. 2D). On the other side, the loss of pCav-1 obtained by Cav-1 knockdown in both the cell lines (Fig. 3A, western blot) determined an impaired proliferative ability, as observed by cell counting (Fig. 3A, bottom graph). In particular, Cav-1 knockdown induced an increase in G1 phase compared to controls (Fig. 3B), indicating a link between Cav-1 and the cell cycle machinery.

pCav-1 levels impact the phosphorylation state of ERK and AKT kinases

We evaluated whether pCav-1 could impact the activation of protein kinase B (known as AKT) and the extracellular regulated kinases (ERK), two critical regulators of cell proliferation and survival in several malignancies [42]. In the RD or RH30 cells, Cav-1 overexpression specifically enhanced the phosphorylation state of either ERK or AKT, respectively, as compared to controls (Fig. 4A, left panels). In addition, the reinforcement of each specific pathway was characterized by the inhibition of the other

one (Fig. 4A, left panels). We were also able to verify that the augmented cell proliferation due to Cav-1 overexpression was consistently overwhelmed by treatment with PD098059 in RD cells or with LY294002 in RH30 cells, two compounds inhibiting the ERK and AKT pathways, respectively (Fig. 4B). On the other side, Cav-1 knockdown determined a down-regulation of pERK and pAKT levels in both the cell lines, though at later time points in RH30 cells (Fig. 4A, right panels), thus suggesting that gain or loss of Cav-1 may impact the activation state of ERK and AKT kinases in a cell-context dependent manner.

pCav-1 promotes cell migration and invasion *in vitro* and tumor growth *in vivo*

By employing a Boyden chamber assay we observed an increased or reduced migration of RD and RH30 cells upon Cav-1 overexpression and silencing compared to controls, respectively (Fig. 5A). Likewise, the increased or decreased Cav-1 levels correlated with the degree of cell invasiveness and activation of the matrix metalloprotease-2 (MMP2) [43], as observed by means of Matrigel and zymography assays performed on RD cells (Fig. 5B and 5C, respectively). In addition, PP2 treatment was sufficient to overwhelm the increased migration (Fig. 5D), invasion (Fig. 5E) and MMP2 activation of Cav-1 overexpressing RD cells (Fig. 5F). We then evaluated the effects of Cav-1 overexpression on tumor growth *in vivo*. To this purpose, mock and Cav-1 overexpressing RD cells were subcutaneously injected into the back of nude mice ($n=8$). Tumor growth was significantly accelerated in mice injected with Cav-1 overexpressing RD cells (Fig. 6A), yielding huge tumor masses characterized by a visible increased vascularization and a weight of about 4 times higher compared to controls (Fig. 6B). As determined by immunohistochemistry, the bigger tumor masses with expectedly high Cav-1 expression were characterized by increased staining with marker of proliferation Ki-67 (MKI67, also known as MIB-1) and cluster of differentiation 31 (CD31), two markers predictive of cell mitosis and vascularization, respectively (Fig. 6C). Of note, we were unable to assess whether the loss of Cav-1 could lead to a regression of tumor growth *in vivo*, because the injected shCav-1 cells had lost the silencing effects yielding tumor masses largely positive for Cav-1 (not shown).

pCav-1 contributes to chemoresistance

Since Cav-1 is long known to play a pivotal role in chemoresistance [44], the cell survival of Cav-1 clones was tested in the presence of chemotherapeutic compounds. In comparison to control cells, Cav-1 overexpressing and knockdown cells were respectively more resistant or sensitized to cell death in response to cisplatin or doxorubicin treatment, as deduced by Crystal violet assay (Fig. 7A). Significantly, the drug resistance of Cav-1 overexpressing cells was almost abolished by co-treatment with PP2 (Fig. 7B), suggesting the contribute of pCav-1 to multidrug resistance. In addition, Cav-1 overexpression and knockdown respectively protected or sensitized cells to a caspase-dependent apoptosis [45], as evaluated by western blot analysis of the active

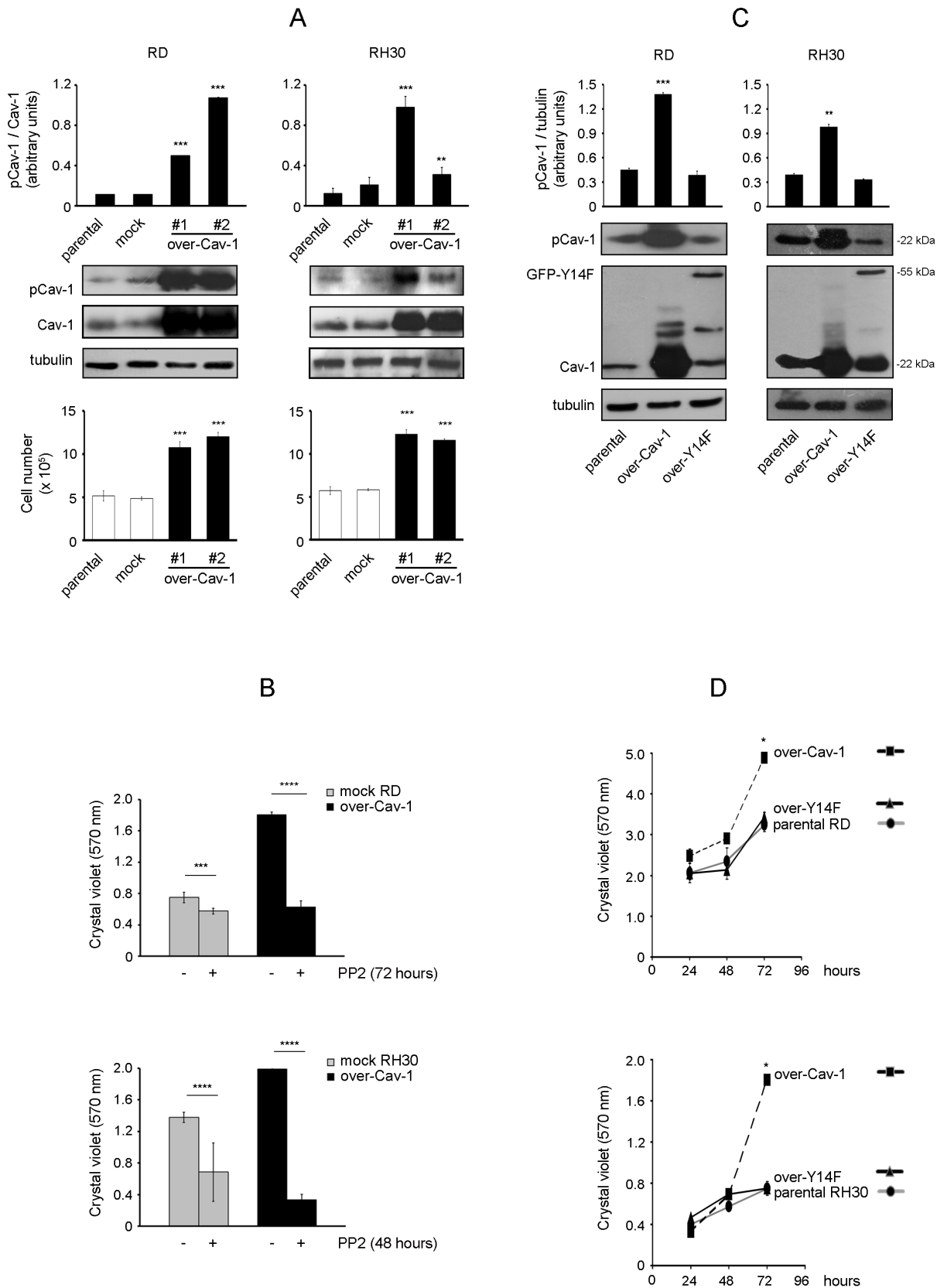


Figure 2. Effects of Cav-1 overexpression on cell proliferation. RD and RH30 cells were stably transfected with either Cav-1 construct (over-Cav-1) or empty vector (mock). A) Parental cells and selected clones were seeded in 60-mm dishes (at a density of 15×10^4). After 48 hours, cells were harvested and protein homogenates western blotted for pCav-1, Cav-1 and tubulin. Protein bands were quantified by densitometry after normalization with respect to tubulin (n=3). **, $P < 0.001$; ***, $P < 0.0001$. At the same time points, cell proliferation was evaluated with Burker

chamber, as shown in the bottom graphs. Bar graphs represent means \pm SD of total cell numbers. ($n = 3$) ***, $P < 0.0001$. B) Mock and over-Cav-1 cells were seeded in 24-well plates (at a density of 15×10^3). After 24 hours, cells were either treated with dimethylsulfoxide (DMSO, vehicle) or 10 μ M PP2 (replenished every 24 or 16 hours for RD and RH30 cells, respectively) for the indicated time points. Cell proliferation was then evaluated by Crystal violet assay. Histograms represent means \pm SD of absorbance ($n = 4$). ***, $P < 0.0001$; ****, $P < 2 \times 10^{-6}$. C) RD and RH30 cells were stably transfected with constructs for either Cav-1 (22 kDa) or non-phosphorylatable GFP-Y14F (55 kDa). Parental cells and selected clones were seeded in 60-mm dishes (at a density of 12×10^4). After 24 hours, cells were harvested and protein homogenates western blotted for pCav-1, Cav-1 and tubulin. Protein bands were quantified by densitometry after normalization with respect to tubulin ($n = 3$). **, $P < 0.001$; ***, $P < 0.0001$. D) Under the same conditions seen above, cell proliferation was evaluated by Crystal violet assay at the indicated time points. Histograms represent means \pm SD of absorbance ($n = 4$). *, $P < 0.05$.
doi:10.1371/journal.pone.0084618.g002

caspase-3 fragments (19 and 17 kDa) (Fig. 7C). This set of experiments shows that overexpression or lack of Cav-1 cooperates to protect from or enhance a caspase-dependent apoptosis in RMS cells, respectively.

Discussion

Cav-1 and *Cav-2* genes are located in a fragile site (known as D7S522 locus) that is frequently deleted in human cancers [46], indicating a common role as tumor suppressors. Consistent with these observations, an impaired Cav-1 expression was found in human lung [47], mammary [48], colon [49] and ovarian carcinomas [50] or sarcomas as well [51]. Cav-1 and Cav-2 conventionally form plasma membrane hetero-oligomers that negatively regulate the activity of several receptors involved in cell proliferation and survival [52–54], and therefore their loss is thought to facilitate tumor progression by deliberate activation of different signaling pathways, as observed in the tumor prone Cav-1 knock-out mouse model [55–59]. Yet, additional mechanisms complicating the scenario have been described, since the inhibitory interaction of Cav-1 with the epidermal growth factor receptor can be hindered by the formation of a galectin-glycoprotein lattice, thereby resulting in sustained receptor activity, as observed in breast tumor cells [60,61]. Beyond functioning as a tumor suppressor, accumulating evidence have more recently indicated that Cav-1, especially when phosphorylated in Tyr14, behaves as an ambiguous partner in cancer [11–15], because of its ability to activate pathways involved in cell migration and invasion, such as the Rho/ROCK and Focal adhesion kinases signaling systems [62]. The data presented here point to pCav-1 as a positive modulator of proliferation, migration, invasiveness, chemoresistance *in vitro* and tumor growth *in vivo* in RMS, the most frequent childhood soft tissue sarcoma characterized by expression of myogenic markers and impaired differentiation [21–28]. The malignant cell phenotype we observed by Cav-1 overexpression was ascribable to the robust increase of Cav-1 phosphorylation in Tyr14, likely due to an increased accessibility of the intracellular Cav-1 pool to Src-family members, as observed in other cellular models [63,64]. In this regard, further studies are required to examine whether and how Cav-1 overexpression may perturb the *caveolae* organization and Cav-1 trafficking in RMS cells. Among its many features, Cav-1 has widely been reported to exert both inhibitory and activatory functions on the RAS/ERK and AKT pathways depending on the cellular context (see for a review [11–15]) and, more recently, pCav1 was found to be specifically interconnected with ERK and AKT signaling in mouse embryonic stem cells [65]. In this context, it is quite of interest that we observed pCav-1 reinforcing the proliferation of the embryonal RD or alveolar RH30 cells via specific increase of either ERK or AKT signaling, respectively, since activating *RAS* mutations leading to sustained ERK signaling are solely detected in ERMS [66–70] and the Pax3-Foxo1 factor strongly cooperates with activated AKT signaling in ARMS malignancy [71,72]. An additional cue of interest was that we

observed pCav-1 cooperating to the overactivation of one specific pathway and causally inhibition of the other one (or *viceversa*). It is largely documented that AKT and ERK signaling influence with each other by positive or negative crosstalks in a cell-context dependent manner [73], and a recent report has shown that if one of these two pathways is chemically inhibited in various RMS cell lines, including RD and RH30 cells, they opportunistically potentiate the other one to survive [74]. Intriguingly, the same authors showed that the block of either pathway did not result in the potentiation of the other one in the RMS TE671 cell line [74], in which we have previously shown the lack of Cav-1 expression [32], therefore cautiously suggesting that Cav-1 may participate to the negative ERK/AKT crosstalk observed in some RMS cells.

Finally, we observed such a clear connection between Cav-1 and the cell cycle machinery of RMS cells, as analogously reported for human endothelial cells [75]. Cav-1 knockdown induced an accumulation in G1 phase and subsequent block of cell proliferation characterized by down-regulation of both ERK and AKT. Thus, the loss of Cav-1 could mimic to some extent the pro-apoptotic effects produced by the concomitant chemical ERK/AKT inhibition [74,76], thereby sensitizing RMS cells to cell death in response to chemotherapeutic agents, definitely pointing to pCav-1 as a therapeutically valuable target to overcome RMS malignancy. In this perspective, since the recent growing body of literature indicating a cooperation between Cav-1 and the polymerase transcription released factor PTRF/Cavin-1 in cancer progression [4,77–85], it will be certainly important to assess their relative contribution in RMS malignancy.

Materials and Methods

All reagents were from Sigma-Aldrich (Milan, Italy), unless otherwise stated.

Ethic statement

This study was carried out in strict accordance with the recommendations in the Guide for the Care and Use of Laboratory Animals of the University of Perugia (Italy). The protocol was approved by the Committee on the Ethics of Animal Experiments of the University of Perugia. All surgery was performed under sodium pentobarbital anesthesia, and all efforts were made to minimize suffering.

Cell culture

Human RD and RH30 cells were purchased from the European Collection of Cell Cultures (ECACC, Salisbury, UK). RD cells harbor *RAS* [86,87] and *P53* [88] mutations, while RH30 cells express Pax3-Foxo1 [89] and harbor *P53* mutations [88]. RD12 and RD18 cell lines were derived by random cloning of the RD line [90,91]. The mouse primary cultures, namely U57810 (ERMS) and U23674 (ARMS), were established from the transgenic Myf6Cre/*p53*^{-/-} and Myf6Cre/*Pax3-Foxo1/p53*^{-/-} mice, respectively [21,24]. Cells were routinely maintained under standard conditions (37°C and 5% CO₂ in humidified incubator)

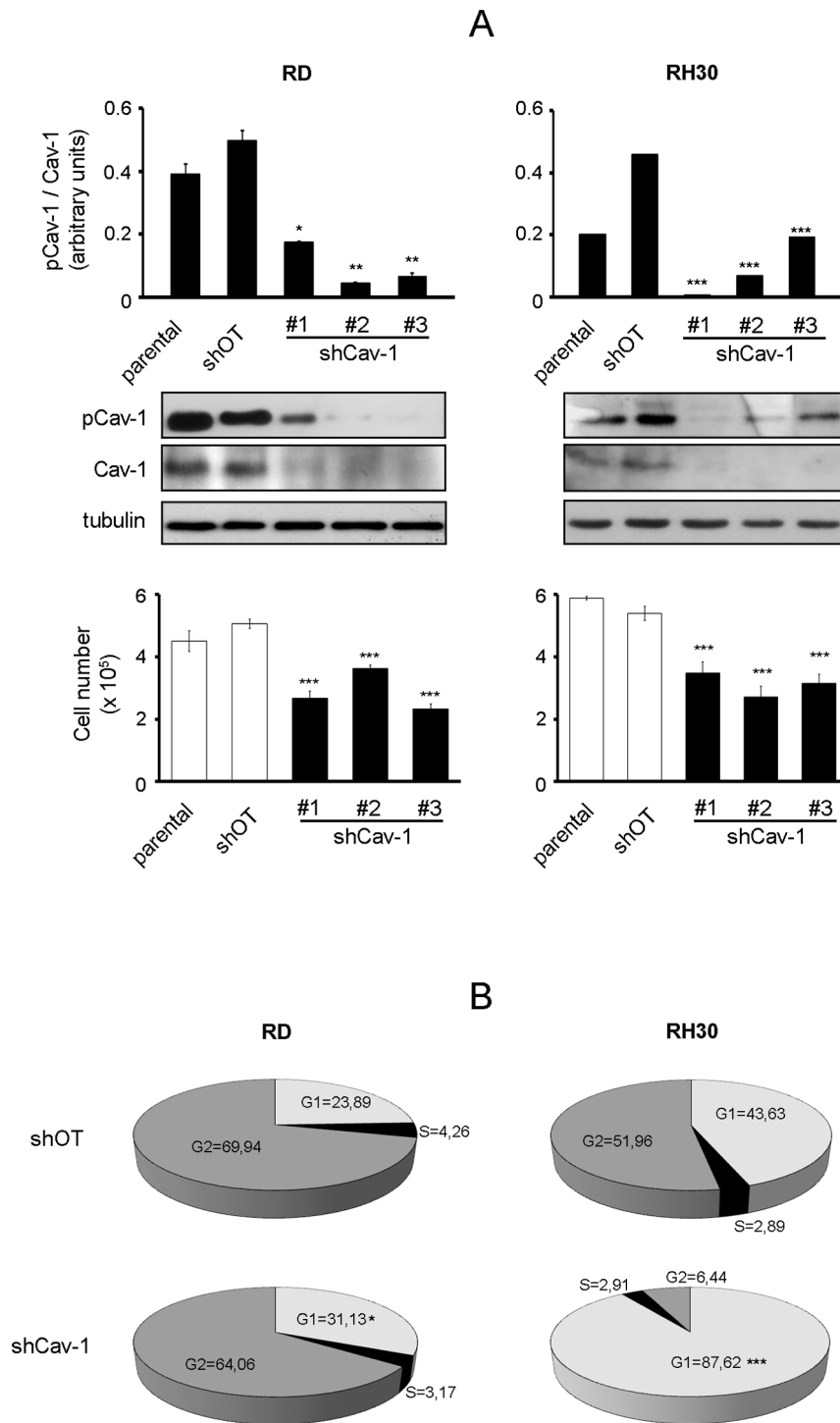


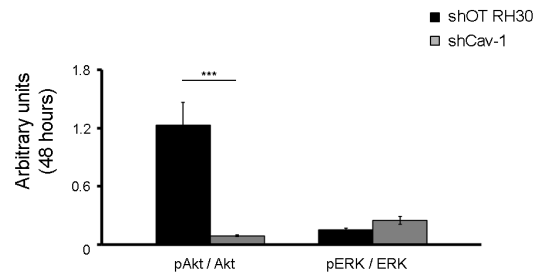
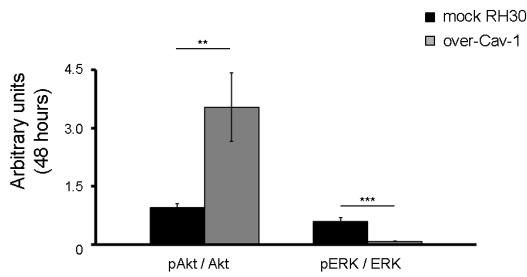
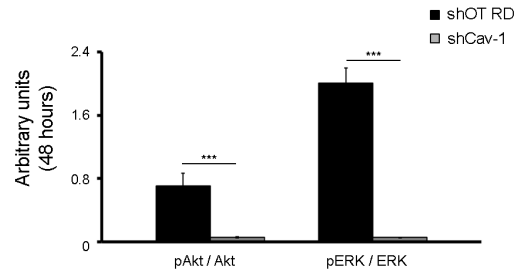
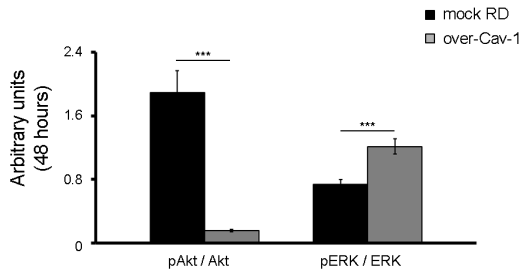
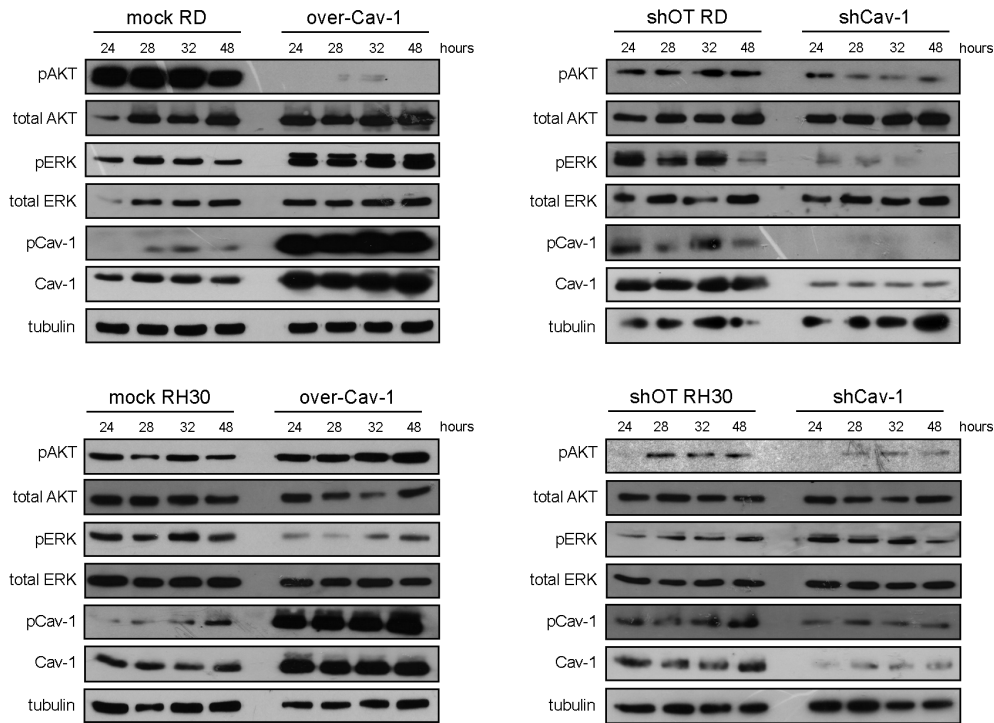
Figure 3. Effects of Cav-1 knockdown on cell proliferation. RD and RH30 cells were stably transfected with either Cav-1 knockdown (shCav-1) or off-target (shOT) construct. A) Parental cells and selected clones were seeded in 60-mm dishes (at a density of 12×10^4). After 48 hours, cells were harvested and protein homogenates western blotted for pCav-1, Cav-1 and tubulin. Protein bands were quantified by densitometry after normalization with respect to tubulin ($n=3$). *, $P<0.05$; **, $P<0.001$; ***, $P<0.0001$. At the same time points, cell proliferation was evaluated with Burkler chamber, as shown in the bottom graphs. Bar graphs represent means \pm SD of total cell numbers ($n=3$). ***, $P<0.0001$. B) FACS analysis was performed on shCav-1 and shOT cells. Numbers in pie charts denote percent cells in the G1/S/G2-phases of the cell cycle ($n=3$). *, $P<0.05$; ***, $P<0.0001$.

doi:10.1371/journal.pone.0084618.g003

in GM, composed by high-glucose Dulbecco's modified eagle's medium (DMEM) supplemented with 10% foetal bovine serum (FBS) in the presence of 100 μ g/ml penicillin/streptomycin

antibiotics and 1% L-Glutamine (only for RH30 cells). To induce myodifferentiation, 80% confluent cells were switched to DM, composed by DMEM supplemented with 2% horse serum. Cells

A



B

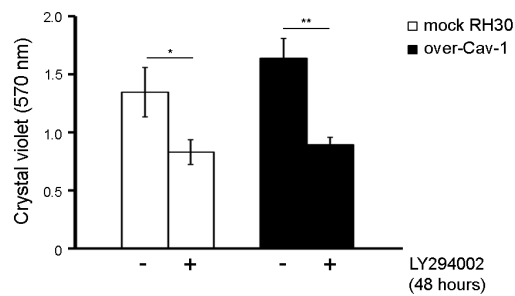
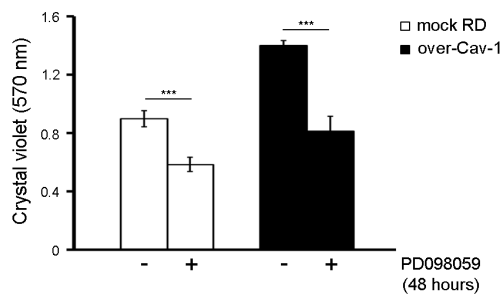


Figure 4. Effects of Cav-1 levels on the phosphorylation state of ERK and AKT. Control, over-Cav-1 cells and shCav-1 cells were seeded in 60-mm dishes (at a density of 12×10^4). A) At the indicated time points, cells were harvested and protein homogenates western blotted for pAKT, AKT, pERK, ERK, pCav-1, Cav-1 and tubulin at the indicated time points. Protein bands corresponding to pAKT and pERK levels (as detected at 48 hours) were quantified by densitometry after normalization with respect to tubulin ($n = 3$). **, $P < 0.001$; ***, $P < 0.0001$. B) 24 hours after seeding, mock and over-Cav-1 cells were treated with 15 μM PD09859 (in the case of RD cell line) or 10 μM LY294002 (in the case of RH30 cell line) for up to 24 hours. Cell proliferation was then evaluated by Crystal violet assay. Histograms represent means \pm SD of absorbance ($n = 4$). *, $P < 0.05$; **, $P < 0.001$; ***, $P < 0.0001$. doi:10.1371/journal.pone.0084618.g004

were treated with: HGF (10 ng/ml, ImmunoTools, Friesoythe, Germany), a Src-kinase inhibitor known as PP2 (10 μM), the chemotherapeutic drugs doxorubicin (0.15 ng/ml) and cisplatin (2 $\mu\text{g}/\text{ml}$), the synthetic inhibitors of the RAS/ERK and AKT cascades, respectively known as PD098059 (15 μM) and LY294002 (10 μM).

Plasmids and transfection

The overexpression of either the wild-type or non-phosphorylatable Cav-1 was carried out by transfection of pCAGGS/Cav-1 (provided by F. Galbiati, University of Pittsburgh, USA) or pEGFPN1/Cav-1(Y14F) (provided by D. Maggi, University of

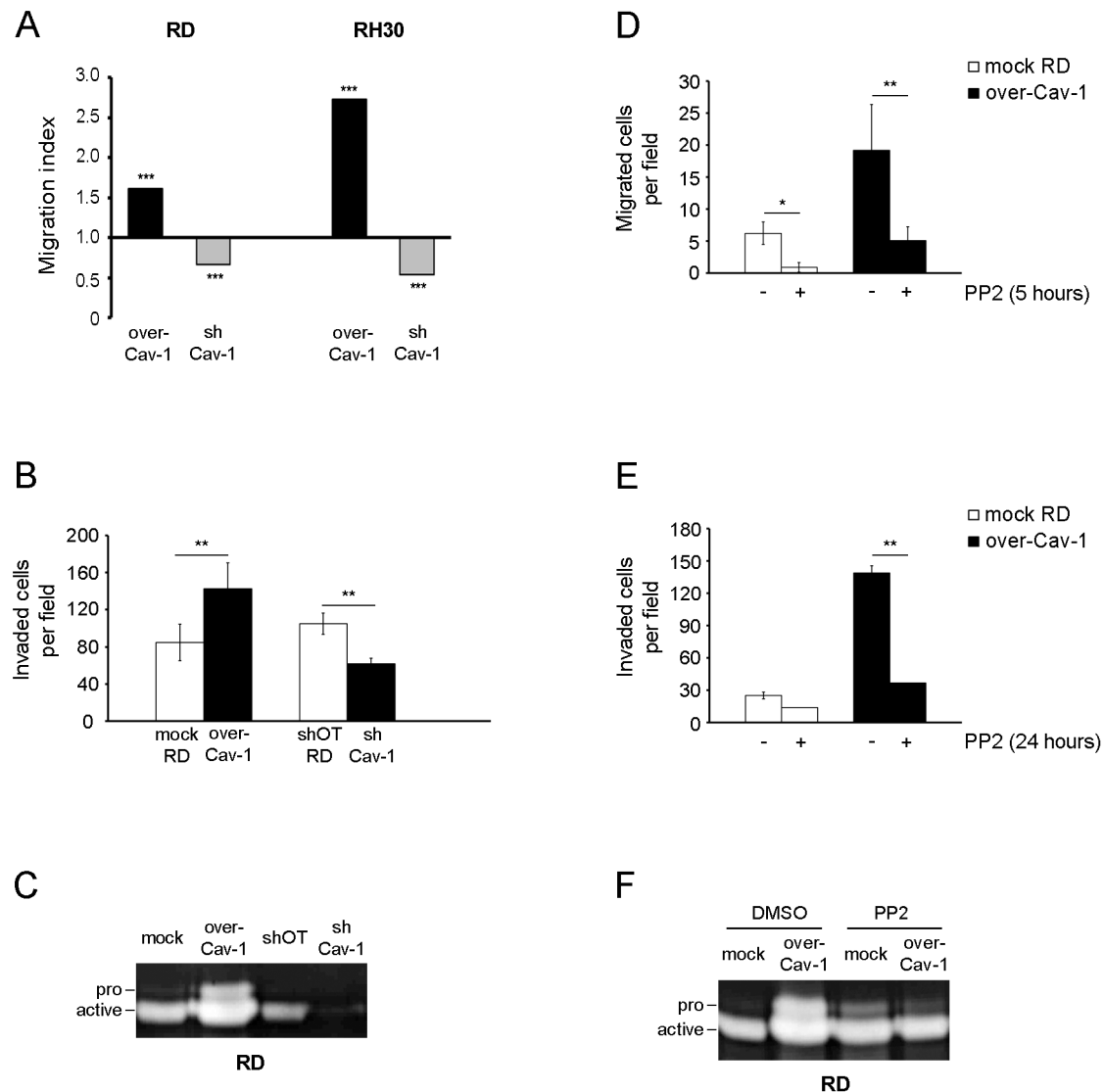


Figure 5. Effects of Cav-1 levels on cell migration and invasiveness. A) Cell migration was evaluated using a modified Boyden chamber assay. The migration index was calculated through the ratio between the mean number of migrated clones (over-Cav-1 and shCav-1) with respect to their migrated controls, as counted in five randomly chosen fields ($n = 3$). ***, $P < 0.0001$. B) Cell invasiveness of RD clones (over-Cav-1 and shCav-1) in comparison to controls was evaluated by Matrigel assay. Histograms represent mean \pm SD ($n = 3$). **, $P < 0.001$. C) Gelatin-zymography assay was performed to evaluate the MMP2 activation in RD clones (over-Cav-1 and shCav-1) with respect to controls. D-E-F) Cell migration (D), invasiveness (E) and the MMP2 activation (F) were evaluated in RD clones (mock and over-Cav-1) treated or not with 10 μM PP2 for 24 hours. Histograms represent means \pm SD ($n = 3$). *, $P < 0.05$; **, $P < 0.001$. doi:10.1371/journal.pone.0084618.g005

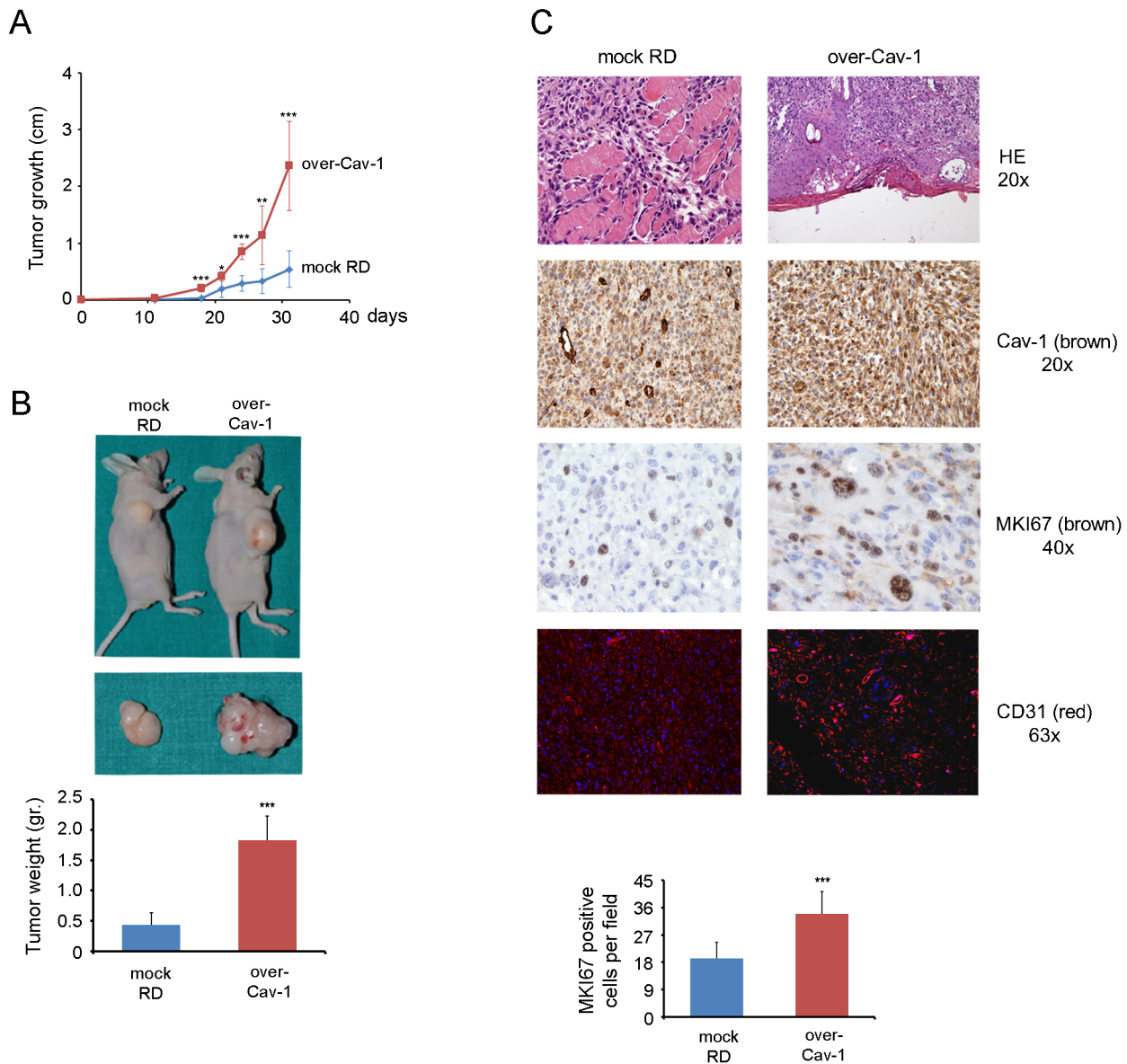


Figure 6. Effects of Cav-1 overexpression on tumor growth *in vivo*. A) Mock and over-Cav-1 RD clones (35×10^5 cells) were subcutaneously injected into the back of nude mice ($n=8$). The size of tumors was measured six times during the subcutaneous growth. Histograms represent means \pm SD of tumor weight. *, $P<0.05$; **, $P<0.001$; ***, $P<0.0001$. B) After 31 days mice were sacrificed and the weight of collected tumors was measured. ***, $P<0.0001$. C) Tumor sections were stained with Hematoxylin and Eosin (HE) and immunostained for Cav-1, MKI67 and CD31. Quantification of MKI67 is reported in the bottom graph. Histograms represent means \pm SD of MKI67 positive cells as counted in five randomly chosen fields. ($n=3$). ***, $P<0.0001$.

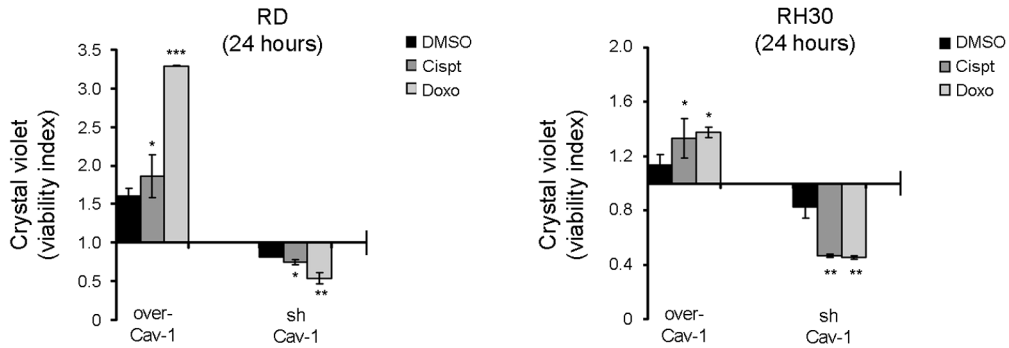
doi:10.1371/journal.pone.0084618.g006

Genova, Italy) constructs, respectively. Knockdown constructs were purchased from Sigma-Aldrich in pLKO.1 backbone: shCav-1 (clone TRCN0000011218), 5'-CCGGGACCCACTCTTTG-AAGCTGTTCTCGAGAACAGCTTCAAAGAGTGGGTCTT-T-3'. As negative controls, pLKO.1-puro harboring the following off-target sequence was used: 5'-CCGGCAACAAGATGAA-GAGCACC AACTCGAGTTGGTGTCTTTCATCTTGTGT-TTTT-3'. Cells were stably transfected using Lipofectamine 2000 reagent (Invitrogen) according to the manufacturer's protocol. After antibiotic selection, the experiments raised similar results in all the selected clones.

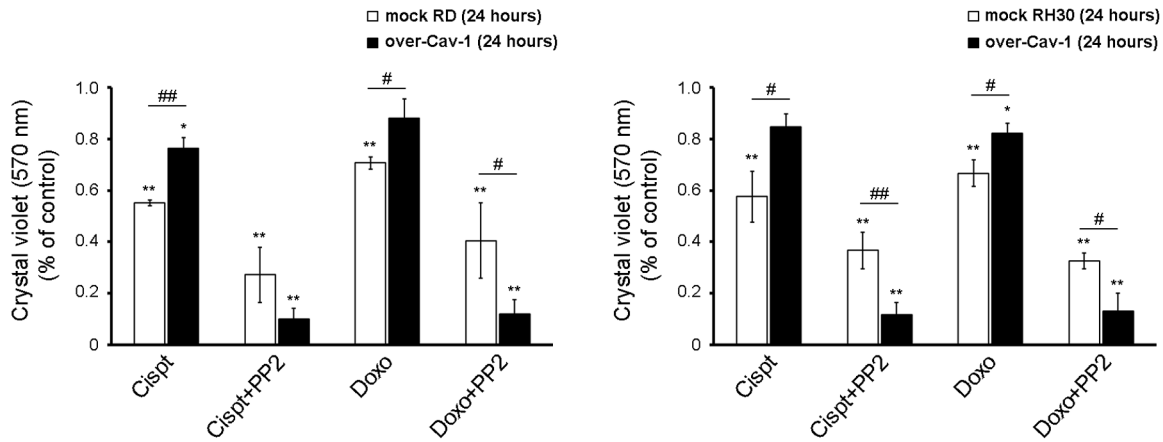
Antibodies

Antibodies used for immunoblotting/immunohistochemistry were phospho-Cav-1 (Tyr14) (code 61338, BD Biosciences, Buccinasco, Italy), Cav-1 (code SC-894, Santa Cruz Biotechnology, Dallas, USA), Cav-2 and Cav-3 (code 610684 and 610420, BD Biosciences, Buccinasco, Italy), phospho-Src (Tyr418) (code 569732, Merck-Millipore, Milan, Italy), total and phospho-AKT (Ser473) (code #2920 and #4060, Cell Signalling, Milan, Italy), total and phospho-ERK (Tyr204) (code SC-135900 and SC-7883, Santa Cruz Biotechnology, Dallas, USA), MKI67 (code NCL-L-Ki67-MM1, Novocastra™ Laboratories Ltd, Newcastle Upon Tyne, United Kingdom), CD31 (code SC-8306, Santa Cruz Biotechnology, Dallas, USA), cleaved Caspase-3 (code #9661,

A



B



C

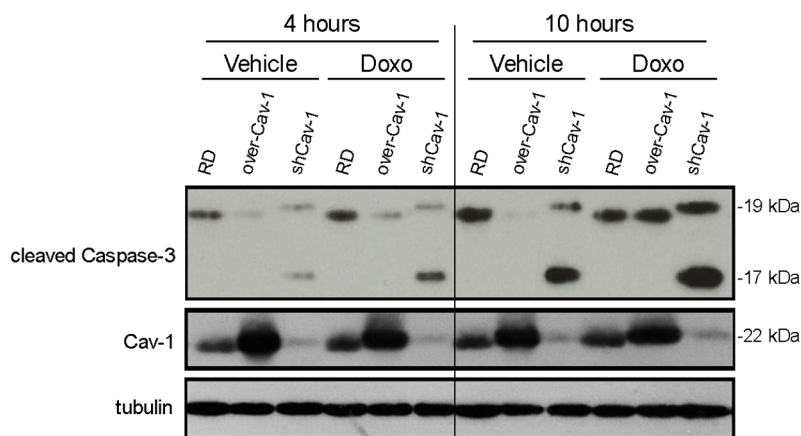


Figure 7. Effects of Cav-1 levels on chemoresistance *in vitro*. A) Cells were seeded into a 24 well plate (at a density of 15×10^3). After 24 hours, cells were treated with cisplatin (0.2 ng/ml) or doxorubicin (2 μ g/ml) and DMSO as control for up to 24 hours. Crystal violet assay was then performed and the viability index was calculated by dividing the mean number of viable cells in Cav-1 overexpressing or silenced clones through their respective controls. Histograms represent means \pm SD of absorbance (n=4). B) Crystal violet assay was carried out to evaluate the percentage of viable Cav-1

overexpressing and control cells after treatment with either cisplatin or doxorubicin in the absence or presence of 10 μ M PP2 for 24 hours. Histograms represent means \pm SD of absorbance (n=4). *, P<0.05; **, P<0.001; ***, P<0.0001 versus untreated cells. #, P<0.05; ##, P<0.001. C) Cleavage of Caspase-3 was evaluated by western blot analysis in over-Cav-1, shCav-1 RD clones and parental cells treated or not with doxorubicin for the indicated time points.
doi:10.1371/journal.pone.0084618.g007

Cell Signalling, Milan, Italy) and tubulin (code T5168, Sigma-Aldrich, Milan, Italy).

Immunoblotting

Protein concentration was calculated by Bradford reagent assay. Equal amounts of protein samples were separated by SDS-PAGE under reducing conditions and transferred to polyvinylidene fluoride membranes. Incubation with specific primary antibodies was followed by horseradish peroxidase-conjugated secondary antibodies (anti-mouse IgG from Santa Cruz Biotechnology, Dallas, USA; anti-rabbit IgG from Thermo Scientific, Erembodegem, Belgium) and the resulting immunocomplexes were visualized using enhanced chemiluminescence reagent (GeneSpin, Milan, Italy). Immunoreactive bands were quantified using densitometric analyses (Software Gel Pro Analyzer, version 4). Total protein homogenates were obtained by harvesting cells in a cold RIPA lysis buffer, composed by 20 mM Tris-HCl (pH 7.6), 1% Nonidet P40, 0.5% sodium deoxycholate, 0.1% SDS, 50 mM NaCl and a cocktail of protease inhibitors (Roche, Milan, Italy) plus phosphatase inhibitors (1 mM Na_3VO_4 and 4 mM NaF). For Caveolin analysis, the Triton-insoluble membranous fractions were obtained by centrifugation of cells harvested in a cold Triton buffer, composed by 10 mM Tris-HCl (pH 8.0), 1% Triton X-100, 5 mM EDTA, 150 mM NaCl, and a cocktail of protease and phosphatase inhibitors (15,000 \times g for 15 minutes at 4°C).

Cell proliferation assay

Cells were seeded in 60-mm dishes (at a density of 15×10^4). After 24, 48 and 72 hours, cells were detached and counted with a Burkner chamber (in triplicate) by a phase contrast microscope. Alternatively, cells were seeded into a 24 well plate (at a density of 15×10^3). After 24, 48 or 72 hours, cells were harvested, paraformaldehyde fixed and stained with Crystal violet (0.5% in PBS with 20% methanol). Absorbance was then measured by reading the plate at 570 nm emission wavelength. Images of cell proliferation assays reflect representative results of at least four independent experiments.

Cell cycle analysis

Cells were seeded in 100-mm dishes (at a density of 70×10^4). After 24 hours, cells were harvested, fixed in 1 ml of ice-cold methanol and stained with 0.5 ml of propidium iodide (100 μ g/ml) containing 5 μ g/ml pancreatic RNase (Agilent Technologies, Wilmington, USA) overnight at 4°C. After gating out cellular aggregates and debris, propidium iodide fluorescence was measured using a CyFlowPartec flow cytometer (Partec Italia, Milan, Italy). Data were analysed with FlowJo software (Tree Star, Ashland, USA).

Chemotaxis assay

Cells (25×10^3 cells in 50 μ l of DMEM with 5% FBS) were seeded in the upper compartment of a Boyden chamber, containing gelatin-coated PVP-free polycarbonate filters (8 μ m pore size, Costar, Cambridge, USA) and DMEM with 10% FBS in the lower compartment. As a negative control, 1% FBS medium was used. After 5 hours of incubation at 37°C, cells migrated to the lower side of the filter were stained with Diff-Quik (Dade-Behring,

Milan, Italy). Five random fields were counted for each triplicate sample.

Matrigel assay

Matrigel assay (BD Biosciences, Buccinasco, Italy) was used to assess the cell invasive potential, according to the manufacturer's protocol. Briefly, cells were plated into upper inserts of 24-well plates (at a density of 60×10^3) and incubated at 37°C. Bottom chambers were filled with 500 μ l of DMEM supplemented with 10% FBS as a chemoattractant or DMEM only as a negative control. After 24 hours, non-invading cells were gently removed from the upper surface of inserts with a cotton swab and invaded cells were methanol fixed and stained with Crystal violet (0.1% in PBS with 20% methanol). The number of cells that invaded the filter was counted using a bright-field microscope. Five randomly selected fields were counted for each filter and experiments were performed in triplicate.

Zymography assay

The activity of MMP2 was assayed by loading 40 μ l of low serum (0.1% FBS) cell conditioned medium into 10% SDS-PAGE containing 1 mg/ml incorporated gelatin substrate. Following electrophoresis, the gels were soaked in 2.5% Triton X-100 to remove SDS and incubated for 24 hours at 37°C in the Collagenase Buffer (50 mM Tris-HCl, 5 mM CaCl_2 , 0.02% Na Azide, 0.005% Brij 35, 1 μ M ZnCl_2) with or without 5 mM EDTA. Clear bands were visualized on the blue background after staining with 0.1% Coomassie blue in 40% ethanol and 10% acetic acid and destained in 30% methanol and 10% acetic acid.

Xenograft experiments

Athymic nude female mice (nu/nu, Harlan Laboratories, Bresso, Italy) weighing ~20 gr were subcutaneously injected with 35×10^5 RD cells in the back. Mice were inspected twice a week and sacrificed by cervical dislocation after 5 weeks. Tumor volume was calculated by the equation: tumor volume = $x^2y/2$, where x and y correspond to the width and thickness of the tissue, respectively. Tumor masses were then excised, weighed and fixed with 10% formalin in PBS (2 days at 4°C), extensively washed in PBS, and paraffin-embedded.

Immunohistochemistry

Immunohistochemistry was performed on paraffin sections according to the manufacturer's protocol. Briefly, sections were de-waxed, re-hydrated and endogenous peroxidase activity blocked by 0.3% H_2O_2 /methanol for 20 minutes. Heat-induced antigen retrieval was performed using a thermostatic bath in 1 mmol/l EDTA (pH 8.0) or 1 mM Citrate buffer (pH 6.0). Sections were then washed in TBS (pH 7.4) and incubated overnight in TBS/1% bovine serum albumin with the specific primary antibody. Single immunostain has been revealed by ChemMATE EnVision HRP Labelled Polymer system (DAKO, Glostrup, Denmark) or NovoLink™ Polymer Detection System (Novocastra™ Laboratories Ltd, Newcastle Upon Tyne, United Kingdom) followed by diaminobenzidine as chromogen and Hematoxylin and Eosin as counterstain.

Statistical analysis

Linear models fitted by ordinary least squares or generalised least squares in case modelling the heteroscedasticity were used. The differences between the groups were analyzed by unpaired Student's *t* test and One-Way ANOVA test (with Dunnett's post-test), using Prism 4 software for Windows (GraphPad Software, San Diego, USA). Statements of significance were based on a *p* value of less than 0.05.

References

- Williams TM, Lisanti MP (2004) The caveolin proteins. *Genome Biol* 5: 214.
- Lajoie P, Nabi IR (2010) Lipid rafts, caveolae, and their endocytosis. *Int Rev Cell Mol Biol* 282: 135–163.
- Parton RG, del Pozo MA (2013) Caveolae as plasma membrane sensors, protectors and organizers. *Nat Rev Mol Cell Biol* 14: 98–112.
- Hill MM, Bastiani M, Luettnerforst R, Kirkham M, Kirkham A, et al. (2008) PTRF-Cavin, a conserved cytoplasmic protein required for caveola formation and function. *Cell* 132: 113–124.
- Hansen CG, Nichols BJ (2010) Exploring the caves: cavins, caveolins and caveolae. *Trends Cell Biol* 20: 177–186.
- Briand N, Dugail I, Le Lay S (2011) Cavin proteins: New players in the caveolae field. *Biochimie* 93: 71–77.
- Boscher C, Nabi IR (2012) Caveolin-1: role in cell signaling. *Adv Exp Med Biol* 729: 29–50.
- Li S, Seitz R, Lisanti MP (1996) Phosphorylation of caveolin by src tyrosine kinases. The alpha-isoform of caveolin is selectively phosphorylated by v-Src in vivo. *J Biol Chem* 271: 3863–3868.
- Volonté D, Galbiati F, Pestell RG, Lisanti MP (2001) Cellular stress induces the tyrosine phosphorylation of caveolin-1 (Tyr¹⁴) via activation of p38 mitogen-activated protein kinase and c-Src kinase. Evidence for caveolae, the actin cytoskeleton, and focal adhesions as mechanical sensors of osmotic stress. *J Biol Chem* 276: 8094–8103.
- Sanguinetti AR, Cao H, Corley Mastick C (2003) Fyn is required for oxidative- and hyperosmotic-stress-induced tyrosine phosphorylation of caveolin-1. *Biochem J* 376: 159–168.
- Quest AF, Lobos-González L, Nuñez S, Sanhueza C, Fernández JG, et al. (2013) The caveolin-1 connection to cell death and survival. *Curr Mol Med* 13: 266–281.
- Burgermeister E, Liscovitch M, Röcken C, Schmid RM, Ebert MP (2008) Caveats of caveolin-1 in cancer progression. *Cancer Lett* 268: 187–201.
- Goetz JG, Lajoie P, Wiseman SM, Nabi IR (2008) Caveolin-1 in tumor progression: the good, the bad and the ugly. *Cancer Metastasis Rev* 27: 715–735.
- Quest AF, Gutierrez-Pajares JL, Torres VA (2008) Caveolin-1: an ambiguous partner in cell signalling and cancer. *J Cell Mol Med* 12: 1130–1150.
- Sáinz-Jaspeado M, Martín-Liberal J, Lagares-Tena L, Mateo-Lozano S, García del Muro X, et al. (2011) Caveolin-1 in sarcomas: friend or foe? *Oncotarget* 2: 305–312.
- Xia SJ, Pressey JG, Barr FG (2002) Molecular pathogenesis of rhabdomyosarcoma. *Cancer Biol Ther* 1: 97–104.
- De Giovanni C, Landuzzi L, Nicoletti G, Lollini PL, Nanni P (2009) Molecular and cellular biology of rhabdomyosarcoma. *Future Oncol* 5: 1449–1475.
- Perez EA, Kassira N, Cheung MC, Koniaris LG, Neville HL, et al. (2011) Rhabdomyosarcoma in children: a SEER population based study. *J Surg Res* 170: e243–251.
- Parham DM, Alaggio R, Coffin CM (2012) Myogenic tumors in children and adolescents. *Pediatr Dev Pathol* 15: 211–238.
- Parham DM, Barr FG (2013) Classification of rhabdomyosarcoma and its molecular basis. *Adv Anat Pathol* 20: 387–397.
- Keller C, Arenkiel BR, Coffin CM, El-Bardeesy N, DePinho RA, et al. (2004) Alveolar rhabdomyosarcomas in conditional Pax3:Fkhr mice: cooperativity of Ink4a/ARF and Trp53 loss of function. *Genes Dev* 18: 2614–2626.
- Linardic CM, Downie DL, Qualman S, Bentley RC, Counter CM (2005) Genetic modeling of human rhabdomyosarcoma. *Cancer Res* 65: 4490–4495.
- Charytonowicz E, Cordon-Cardo C, Matushansky I, Ziman M (2009) Alveolar rhabdomyosarcoma: is the cell of origin a mesenchymal stem cell? *Cancer Lett* 279: 126–136.
- Rubin BP, Nishijo K, Chen HI, Yi X, Schuetz DP, et al. (2011) Evidence for an unanticipated relationship between undifferentiated pleomorphic sarcoma and embryonal rhabdomyosarcoma. *Cancer Cell* 19: 177–191.
- Rodríguez R, Rubio R, Menendez P (2012) Modeling sarcomagenesis using multipotent mesenchymal stem cells. *Cell Res* 22: 62–77.
- Zanola A, Rossi S, Faggi F, Monti E, Fanzani A (2012) Rhabdomyosarcomas: an overview on the experimental animal models. *J Cell Mol Med*.
- Fanzani A, Monti E, Donato R, Sorci G (2013) Muscular dystrophies share pathogenetic mechanisms with muscle sarcomas. *Trends Mol Med* 19: 546–554.

Acknowledgments

We are grateful to Charles Keller (Oregon and Health University, USA) for providing the primary mouse tumor cultures.

Author Contributions

Conceived and designed the experiments: AF FF SM GS RD EM. Performed the experiments: FF SM GS FR S. Codenotti PLP M. Cominelli RV SR IP. Analyzed the data: AF FF SM GS RD EM. Contributed reagents/materials/analysis tools: M. Colombi FP PC MS. Wrote the paper: AF. Performed the statistical analysis: S. Calza.

- Keller C, Guttridge DC (2013) Mechanisms of impaired differentiation in rhabdomyosarcoma. *FEBS J* 280: 4323–4334.
- Marshall AD, Grosveld GC (2012) Alveolar rhabdomyosarcoma - The molecular drivers of PAX3/7-FOXO1-induced tumorigenesis. *Skelet Muscle* 2: 25.
- Olanich ME, Barr FG (2013) A call to ARMS: targeting the PAX3-FOXO1 gene in alveolar rhabdomyosarcoma. *Expert Opin Ther Targets* 17: 607–623.
- Rossi S, Poliani PL, Cominelli M, Bozzato A, Vescovi R, et al. (2011) Caveolin 1 is a marker of poor differentiation in Rhabdomyosarcoma. *Eur J Cancer* 47: 761–772.
- Rossi S, Poliani PL, Missale C, Monti E, Fanzani A (2011) Caveolins in rhabdomyosarcoma. *J Cell Mol Med* 15: 2553–2568.
- Shor AC, Keselman EA, Lee FY, Muro-Cacho C, Letson GD, et al. (2007) Dasatinib inhibits migration and invasion in diverse human sarcoma cell lines and induces apoptosis in bone sarcoma cells dependent on SRC kinase for survival. *Cancer Res* 67: 2800–2808.
- Taniguchi E, Nishijo K, McCleish AT, Michalek JE, Grayson MH, et al. (2008) PDGFR-A is a therapeutic target in alveolar rhabdomyosarcoma. *Oncogene* 27: 6550–6560.
- Croise LE, Linardic CM (2011) Receptor tyrosine kinases as therapeutic targets in rhabdomyosarcoma. *Sarcoma* 2011: 756982.
- Bai Y, Li J, Fang B, Edwards A, Zhang G, et al. (2012) Phosphoproteomics identifies driver tyrosine kinases in sarcoma cell lines and tumors. *Cancer Res* 72: 2501–2511.
- Abraham J, Chua YX, Glover JM, Tyner JW, Loriaux MM, et al. (2012) An adaptive Src-PDGFRα-Raf axis in rhabdomyosarcoma. *Biochem Biophys Res Commun* 426: 363–368.
- Sharp R, Recio JA, Jhappan C, Otsuka T, Liu S, et al. (2002) Synergism between Ink4a/ARF inactivation and aberrant HGF/SF signaling in rhabdomyosarcomagenesis. *Nat Med* 8: 1276–1280.
- Jankowski K, Kucia M, Wysoczynski M, Reza R, Zhao D, et al. (2003) Both hepatocyte growth factor (HGF) and stromal-derived factor-1 regulate the metastatic behavior of human rhabdomyosarcoma cells, but only HGF enhances their resistance to radiochemotherapy. *Cancer Res* 63: 7926–7935.
- Taulli R, Scuoppo C, Bersani F, Accornero P, Forni PE, et al. (2006) Validation of met as a therapeutic target in alveolar and embryonal rhabdomyosarcoma. *Cancer Res* 66: 4742–4749.
- Hinson AR, Jones R, Croise LE, Belyea BC, Barr FG, et al. (2013) Human rhabdomyosarcoma cell lines for rhabdomyosarcoma research: utility and pitfalls. *Front Oncol* 3: 183.
- De Luca A, Maiello MR, D'Alessio A, Pergameno M, Normanno N (2012) The RAS/RAF/MEK/ERK and the PI3K/AKT signalling pathways: role in cancer pathogenesis and implications for therapeutic approaches. *Expert Opin Ther Targets* 16 Suppl 2: S17–27.
- Onisto M, Slongo ML, Gregnanin L, Gastaldi T, Carli M, et al. (2005) Expression and activity of vascular endothelial growth factor and metalloproteinases in alveolar and embryonal rhabdomyosarcoma cell lines. *Int J Oncol* 27: 791–798.
- Hehlgans S, Cordes N (2011) Caveolin-1: an essential modulator of cancer cell radio- and chemoresistance. *Am J Cancer Res* 1: 521–530.
- Galluzzi L, Vitale I, Abrams JM, Alnemri ES, Bachrecke EH, et al. (2012) Molecular definitions of cell death subroutines: recommendations of the Nomenclature Committee on Cell Death 2012. *Cell Death Differ* 19: 107–120.
- Engelman JA, Zhang XL, Lisanti MP (1998) Genes encoding human caveolin-1 and -2 are co-localized to the D7S522 locus (7q31.1), a known fragile site (FRA7G) that is frequently deleted in human cancers. *FEBS Lett* 436: 403–410.
- Racine C, Bélanger M, Hirabayashi H, Boucher M, Chakir J, et al. (1999) Reduction of caveolin 1 gene expression in lung carcinoma cell lines. *Biochem Biophys Res Commun* 255: 580–586.
- Lee SW, Reimer CL, Oh P, Campbell DB, Schnitzer JE (1998) Tumor cell growth inhibition by caveolin re-expression in human breast cancer cells. *Oncogene* 16: 1391–1397.
- Bender FC, Raymond MA, Bron C, Quest AF (2000) Caveolin-1 levels are down-regulated in human colon tumors, and ectopic expression of caveolin-1 in colon carcinoma cell lines reduces cell tumorigenicity. *Cancer Res* 60: 5870–5878.

50. Wiechen K, Diatchenko L, Agoulnik A, Scharff KM, Schober H, et al. (2001) Caveolin-1 is down-regulated in human ovarian carcinoma and acts as a candidate tumor suppressor gene. *Am J Pathol* 159: 1635–1643.
51. Wiechen K, Sers C, Agoulnik A, Arlt K, Dietel M, et al. (2001) Down-regulation of caveolin-1, a candidate tumor suppressor gene, in sarcomas. *Am J Pathol* 158: 833–839.
52. Razani B, Zhang XL, Bitzer M, von Gersdorff G, Böttinger EP, et al. (2001) Caveolin-1 regulates transforming growth factor (TGF)-beta/SMAD signaling through an interaction with the TGF-beta type I receptor. *J Biol Chem* 276: 6727–6738.
53. Matveev SV, Smart EJ (2002) Heterologous desensitization of EGF receptors and PDGF receptors by sequestration in caveolae. *Am J Physiol Cell Physiol* 282: C935–946.
54. Di Guglielmo GM, Le Roy C, Goodfellow AF, Wrana JL (2003) Distinct endocytic pathways regulate TGF-beta receptor signalling and turnover. *Nat Cell Biol* 5: 410–421.
55. Drab M, Verkade P, Elger M, Kasper M, Lohn M, et al. (2001) Loss of caveolae, vascular dysfunction, and pulmonary defects in caveolin-1 gene-disrupted mice. *Science* 293: 2449–2452.
56. Razani B, Engelman JA, Wang XB, Schubert W, Zhang XL, et al. (2001) Caveolin-1 null mice are viable but show evidence of hyperproliferative and vascular abnormalities. *J Biol Chem* 276: 38121–38138.
57. Capozza F, Williams TM, Schubert W, McClain S, Bouzahzah B, et al. (2003) Absence of caveolin-1 sensitizes mouse skin to carcinogen-induced epidermal hyperplasia and tumor formation. *Am J Pathol* 162: 2029–2039.
58. Williams TM, Cheung MW, Park DS, Razani B, Cohen AW, et al. (2003) Loss of caveolin-1 gene expression accelerates the development of dysplastic mammary lesions in tumor-prone transgenic mice. *Mol Biol Cell* 14: 1027–1042.
59. Lin MI, Yu J, Murata T, Sessa WC (2007) Caveolin-1-deficient mice have increased tumor microvascular permeability, angiogenesis, and growth. *Cancer Res* 67: 2849–2856.
60. Lajoie P, Partridge EA, Guay G, Goetz JG, Pawling J, et al. (2007) Plasma membrane domain organization regulates EGFR signaling in tumor cells. *J Cell Biol* 179: 341–356.
61. Boscher C, Dennis JW, Nabi IR (2011) Glycosylation, galectins and cellular signaling. *Curr Opin Cell Biol* 23: 383–392.
62. Joshi B, Strugnell SS, Goetz JG, Kojic LD, Cox ME, et al. (2008) Phosphorylated caveolin-1 regulates Rho/ROCK-dependent focal adhesion dynamics and tumor cell migration and invasion. *Cancer Res* 68: 8210–8220.
63. Hayer A, Stoeber M, Ritz D, Engel S, Meyer HH, et al. (2010) Caveolin-1 is ubiquitinated and targeted to intraluminal vesicles in endolysosomes for degradation. *J Cell Biol* 191: 615–629.
64. Hanson CA, Drake KR, Baird MA, Han B, Kraft IJ, et al. (2013) Overexpression of caveolin-1 is sufficient to phenocopy the behavior of a disease-associated mutant. *Traffic* 14: 663–677.
65. Park JH, Han HJ (2009) Caveolin-1 plays important role in EGF-induced migration and proliferation of mouse embryonic stem cells: involvement of PI3K/Akt and ERK. *Am J Physiol Cell Physiol* 297: C935–944.
66. Marampon F, Ciccarelli C, Zani BM (2006) Down-regulation of c-Myc following MEK/ERK inhibition halts the expression of malignant phenotype in rhabdomyosarcoma and in non muscle-derived human tumors. *Mol Cancer* 5: 31.
67. Langenau DM, Keefe MD, Storer NY, Guyon JR, Kutok JL, et al. (2007) Effects of RAS on the genesis of embryonal rhabdomyosarcoma. *Genes Dev* 21: 1382–1395.
68. Marampon F, Bossi G, Ciccarelli C, Di Rocco A, Sacchi A, et al. (2009) MEK/ERK inhibitor U0126 affects in vitro and in vivo growth of embryonal rhabdomyosarcoma. *Mol Cancer Ther* 8: 543–551.
69. Schaaf G, Hamdi M, Zwijnenburg D, Lakeman A, Geerts D, et al. (2010) Silencing of SPRY1 triggers complete regression of rhabdomyosarcoma tumors carrying a mutated RAS gene. *Cancer Res* 70: 762–771.
70. Storer NY, White RM, Uong A, Price E, Nielsen GP, et al. (2013) Zebrafish rhabdomyosarcoma reflects the developmental stage of oncogene expression during myogenesis. *Development* 140: 3040–3050.
71. Petricoin EF, Espina V, Araujo RP, Midura B, Yeung C, et al. (2007) Phosphoprotein pathway mapping: Akt/mammalian target of rapamycin activation is negatively associated with childhood rhabdomyosarcoma survival. *Cancer Res* 67: 3431–3440.
72. Jothi M, Nishijo K, Keller C, Mal AK (2012) AKT and PAX3-FKHR cooperation enforces myogenic differentiation blockade in alveolar rhabdomyosarcoma cell. *Cell Cycle* 11: 895–908.
73. Aksamitiene E, Kiyatkin A, Kholodenko BN (2012) Cross-talk between mitogenic Ras/MAPK and survival PI3K/Akt pathways: a fine balance. *Biochem Soc Trans* 40: 139–146.
74. Guenther MK, Graab U, Fulda S (2013) Synthetic lethal interaction between PI3K/Akt/mTOR and Ras/MEK/ERK pathway inhibition in rhabdomyosarcoma. *Cancer Lett* 337: 200–209.
75. Madaro L, Antonangeli F, Favia A, Esposito B, Biamonte F, et al. (2013) Knock down of caveolin-1 affects morphological and functional hallmarks of human endothelial cells. *J Cell Biochem* 114: 1843–1851.
76. Renshaw J, Taylor KR, Bishop R, Valenti M, De Haven Brandon A, et al. (2013) Dual Blockade of the PI3K/AKT/mTOR (AZD8055) and RAS/MEK/ERK (AZD6244) Pathways Synergistically Inhibits Rhabdomyosarcoma Cell Growth In Vitro and In Vivo. *Clin Cancer Res* 19: 5940–5951.
77. Liu L, Pilch PF (2008) A critical role of cavin (polymerase I and transcript release factor) in caveolae formation and organization. *J Cell Biol* 199: 425–435.
78. Aung CS, Hill MM, Bastiani M, Parton RG, Parat MO (2011) PTRF-cavin-1 expression decreases the migration of PC3 prostate cancer cells: role of matrix metalloproteinase 9. *Eur J Cell Biol* 90: 136–142.
79. Joshi B, Bastiani M, Strugnell SS, Boscher C, Parton RG, et al. (2012) Phosphocaveolin-1 is a mechanotransducer that induces caveola biogenesis via Egr1 transcriptional regulation. *J Cell Biol* 199: 425–435.
80. Bai L, Deng X, Li Q, Wang M, An W, et al. (2012) Down-regulation of the cavin family proteins in breast cancer. *J Cell Biochem* 113: 322–328.
81. Gámez-Pozo A, Sánchez-Navarro I, Calvo E, Agulló-Ortuño MT, López-Vacas R, et al. (2012) PTRF/cavin-1 and MIF proteins are identified as non-small cell lung cancer biomarkers by label-free proteomics. *PLoS One* 7: e33752.
82. Hill MM, Daud NH, Aung CS, Loo D, Martin S, et al. (2012) Co-regulation of cell polarization and migration by caveolar proteins PTRF/Cavin-1 and caveolin-1. *PLoS One* 7: e43041.
83. Inder KL, Zheng YZ, Davis MJ, Moon H, Loo D, et al. (2012) Expression of PTRF in PC-3 Cells modulates cholesterol dynamics and the actin cytoskeleton impacting secretion pathways. *Mol Cell Proteomics* 11: M111.012245.
84. Yi JS, Mun DG, Lee H, Park JS, Lee JW, et al. (2013) PTRF/Cavin-1 is Essential for Multidrug Resistance in Cancer Cells. *J Proteome Res*.
85. Liu L, Xu HX, Wang WQ, Wu CT, Chen T, et al. (2013) Cavin-1 is essential for the tumor-promoting effect of caveolin-1 and enhances its prognostic potency in pancreatic cancer. *Oncogene*.
86. Chardin P, Yeramian P, Madaule P, Tavittian A (1985) N-ras gene activation in the RD human rhabdomyosarcoma cell line. *Int J Cancer* 35: 647–652.
87. Stratton MR, Fisher C, Gusterson BA, Cooper CS (1989) Detection of point mutations in N-ras and K-ras genes of human embryonal rhabdomyosarcomas using oligonucleotide probes and the polymerase chain reaction. *Cancer Res* 49: 6324–6327.
88. Felix CA, Kappel CC, Mitsudomi T, Nau MM, Tsokos M, et al. (1992) Frequency and diversity of p53 mutations in childhood rhabdomyosarcoma. *Cancer Res* 52: 2243–2247.
89. Douglass EC, Valentine M, Etcubanas E, Parham D, Webber BL, et al. (1987) A specific chromosomal abnormality in rhabdomyosarcoma. *Cytogenet Cell Genet* 45: 148–155.
90. Lollini PL, De Giovanni C, Landuzzi L, Nicoletti G, Scotlandi K, et al. (1991) Reduced metastatic ability of in vitro differentiated human rhabdomyosarcoma cells. *Invasion Metastasis* 11: 116–124.
91. Astolfi A, De Giovanni C, Landuzzi L, Nicoletti G, Ricci C, et al. (2001) Identification of new genes related to the myogenic differentiation arrest of human rhabdomyosarcoma cells. *Gene* 274: 139–149.